Compact distributed fiber SPR sensor based on TDM and WDM technology

Zhihai Liu,[1,2] Yong Wei[1], Yu Zhang,[1,2,*] Chunlan Liu,[1] Yaxun Zhang,[1] Enming Zhao,[1] Jun Yang,[1] and Libo Yuan[1]

[1]*Key Lab of In-fiber Integrated Optics, Ministry Education of China, Harbin Engineering University, Harbin 150001, China*

[2]*Centre for Micro-Photonics Swinburne University of Technology, P.O. Box 218 Hawthorn, VIC 3122, Australia*

[*]*zhangy0673@163.com*

Abstract: By using a twin-core fiber (TCF), we propose and demonstrate a novel distributed SPR sensor, which employs both the time division multiplexing (TDM) technology and the wavelength division multiplexing (WDM) technology together. The proposed sensor has two sensing passages with four sensing channels (and there are two sensing channels in each sensing passage). We employ the TDM technology to realize the two passage distributed sensing, which are parallel-connection; and we employ the WDM technology to realize the distributed sensing of two channels in a sensing passage, which are series-connected. In order to realize the TDM technology, we employ a two-core fiber, which has two cores in a same cladding, being equal to dividing the traditional single core into two independent sensing zones; in order to realize the WDM technology, we employ a fiber end polishing-connecting method to adjust the resonance angle/wavelength to realize the dynamic range separation. This twin-passage four-channel twin-core fiber SPR sensor is suitable for applying in fields of the multi-channel liquid refractive index and temperature self-reference measurement.

© 2015 Optical Society of America

OCIS codes: (060.2370) Fiber optics sensors; (060.4005) Microstructured fibers; (130.3990) Micro-optical devices.

References and links

1. K. Nomura, S. C. B. Gopinath, T. Lakshmipriya, N. Fukuda, X. Wang, and M. Fujimaki, "An angular fluidic channel for prism-free surface-plasmon-assisted fluorescence capturing," Nat. Commun. **4**, 2855 (2013).
2. J. H. Ahn, T. Y. Seong, W. M. Kim, T. S. Lee, I. Kim, and K. S. Lee, "Fiber-optic waveguide coupled surface plasmon resonance sensor," Opt. Express **20**(19), 21729–21738 (2012).
3. J. Banerjee, M. Bera, and M. Ray, "Simultaneous excitation of multi-spectral surface plasmon resonance using multi-stepped-thickness metallic film," J. Appl. Phys. **117**(11), 113102 (2015).
4. C. L. Wong and M. Olivo, "Surface Plasmon Resonance Imaging Sensors: A Review," Plasmonics **9**(4), 809–824 (2014).
5. C. E. H. Berger, T. A. M. Beumer, R. P. H. Kooyman, and J. Greve, "Surface Plasmon Resonance Multisensing," Anal. Chem. **70**(4), 703–706 (1998).
6. G. G. Nenninger, J. B. Clendenning, C. E. Furlong, and S. S. Yee, Sens. "Reference-compensated biosensing using a dual-channel surface plasmon resonance sensor system based on a planar lightpipe configuration," Sens. Actuators B Chem. **51**(1–3), 38–45 (1998).
7. J. Homola, H. B. Lu, G. G. Nenninger, J. Dostalek, and S. S. Yee, "A novel multichannel surface plasmon resonance biosensor," Sens. Actuators B Chem. **76**(1–3), 403–410 (2001).
8. J. Dostálek, H. Vaisocherova, and J. Homola, "Multichannel surface plasmon resonance biosensor with wavelength division multiplexing," Sens. Actuators B Chem. **108**(1–2), 758–764 (2005).
9. J. Homola, H. Vaisocherová, J. Dostálek, and M. Piliarik, "Multi-analyte surface plasmon resonance biosensing," Methods **37**(1), 26–36 (2005).
10. J. Homola, J. Dostálek, S. Chen, A. Rasooly, S. Jiang, and S. S. Yee, "Spectral surface plasmon resonance biosensor for detection of staphylococcal enterotoxin B in milk," Int. J. Food Microbiol. **75**(1-2), 61–69 (2002).
11. G. G. Nenninger, J. B. Clendenning, C. E. Furlong, and S. S. Yee, "Reference-compensated biosensing using a dual-channel surface plasmon resonance sensor system based on a planar lightpipe configuration," Sensor. Actuat.

#246622 Received 28 Jul 2015; revised 31 Aug 2015; accepted 1 Sep 2015; published 3 Sep 2015
(C) 2015 OSA

B-Chem. **51**(1–3), 38–45 (1998).
12. Y. C. Kim, W. Peng, S. Banerji, and K. S. Booksh, "Tapered fiber optic surface plasmon resonance sensor for analyses of vapor and liquid phases," Opt. Lett. **30**(17), 2218–2220 (2005).
13. Y. Q. Yuan, L. Wang, and J. Huang, "Theoretical investigation for two cascaded SPR fiber optic sensors," Sensor. Actuat B-Chem. **161**(1), 269–273 (2012).
14. W. Peng, S. Banerji, Y. C. Kim, and K. S. Booksh, "Investigation of dual-channel fiber-optic surface plasmon resonance sensing for biological applications," Opt. Lett. **30**(22), 2988–2990 (2005).
15. Z. Y. Zhang, P. Zhao, F. G. Sun, G. Z. Xiao, and Y. M. Wu, "Self-Referencing in Optical-Fiber Surface Plasmon Resonance Sensors," IEEE Photon. Tech. Lett. **19**(24), 1958–1960 (2007).
16. B. Špačková, M. Piliarik, P. Kvasnička, C. Themistos, M. Rajarajan, and J. Homola, "Novel concept of multi-channel fiber optic surface plasmon resonance sensor," Sensor. Actuat B-Chem. **139**(1), 199–203 (2009).
17. M. D. Baiad and R. Kashyap, "Concatenation of surface plasmon resonance sensors in a single optical fiber using tilted fiber Bragg gratings," Opt. Lett. **40**(1), 115–118 (2015).
18. L. A. Obando and K. S. Booksh, "Tuning Dynamic Range and Sensitivity of White-Light, Multimode, Fiber-Optic Surface Plasmon Resonance Sensors," Anal. Chem. **71**(22), 5116–5122 (1999).
19. Y. Q. Yuan, D. Hu, L. Hua, and M. Li, "Theoretical investigations for surface plasmon resonance based optical fiber tip sensor," Sensor. Actuat B-Chem. **188**(11), 757–760 (2013).
20. R. C. Jorgenson and S. S. Yee, "Control of the dynamic range and sensitivity of a surface plasmon resonance based fiber optic sensor," Sens. Actuators A Phys. **43**(1–3), 44–48 (1994).
21. Y. C. Kim, J. F. Masson, and K. S. Booksh, "Single-crystal sapphire-fiber optic sensors based on surface plasmon resonance spectroscopy for in situ monitoring," Talanta **67**(5), 908–917 (2005).
22. P. B. Johnson and R. W. Christy, "Optical Constants of the Noble Metals," Phys. Rev. B **6**(12), 4370–4379 (1972).

1. Introduction

Surface plasmon resonance (SPR) is a popular surface analysis method used to detect changes in the refractive index or thickness of an adsorbed layer on or near a SPR-active surface with high sensitivity [1–4]. With the development of SPR sensing, multichannel SPR sensors have attracted attention owing to their potential uses in multianalyte detection [5,6].

According to Jiří Homola [7–9], in the prism-based SPR sensors based on spectroscopy analysis, time division multiplexing (TDM) technology and wavelength division multiplexing technology (WDM) are two common methods to realize the multi-channel distributed sensing. In the SPR sensors with wavelength modulation, the TDM technology employs spectral analysis of multiple light beams performed by multiple spectrographs [10] or uses an optical switch routing light from multiple channels at single spectrograph [11]. The WDM technology combines pairs of sensing channel with multi parallel light beams to provide multi sensing channels [7]. In another word, TDM technology realizes multichannel sensing by "parallel connecting" several single-channel sensors; and WDM technology realizes multichannel sensing by "series connecting" multi single-channel sensors.

Compared with prism-based SPR sensor, the fiber-based SPR sensors are fundamentally simpler in construction, are less costly, require a smaller sample volume, and much more amenable for remote sensing applications. However the fiber-based SPR sensor faces the challenges and difficulties to realize the multichannel distributed sensing. For TDM technology, it is not suitable for the fiber-based SPR sensor. The reason is that it is too hard to divide multi parallel zones in a such small fiber core to obtain multi independent sensing zones to realize the "parallel connection", therefore, as far as we know, there is no report about the single fiber SPR sensor based on the TDM technology. For WDM technology, it is also hard to realize the multichannel sensing. The reason is that it is hard to produce two resonance wavelengths with a greater difference in a same spectrograph, which means it is hard to separate two dynamic ranges between two sensing channels to realize the "series connection". Although there are some previous methods realizing the multichannel sensing based on the fiber [12–21], including adopting different kinds and moderate thicknesses of metal layers or polymerized films, but the disadvantage lies in they will undergo the defect of some specific testing wavelength ranges and low sensitivity.

In order to solve this problem, by using a twin-core fiber, we propose and demonstrate a novel fiber-based SPR sensor, which employs both the TDM technology and WDM technology simultaneously. The proposed sensor has two sensing passages with four sensing channels.

#246622 Received 28 Jul 2015; revised 31 Aug 2015; accepted 1 Sep 2015; published 3 Sep 2015
(C) 2015 OSA

Exactly speaking, there are two sensing channels in each sensing passage. We employ the TDM technology to realize the distributed sensing between two parallel-connection passages, and we employ the WDM technology to realize the distributed sensing between two channels series-connected in a passage. In order to realize the TDM technology, we employ a two-core fiber, which has two cores in a same cladding, being equal to dividing the traditional single core into two independent sensing zones, realizing parallel connection; in order to realize the WDM technology, we employ a fiber grinding and buffer-joint connecting method to adjust the SPR resonance angle and resonance wavelength to realize the dynamic range separation, realizing series connection.

2. Principle

2.1 Realization of WDM (series-connection sensor)

In order to realize the WDM technology applied in the distributed fiber-based SPR sensor, which means realizing the series connection of two sensing channels, we propose a fiber end polishing and then butt-joint connecting method.

Sensing zone fabrication: The SPR coupling wavelength can be tuned selectively by modifying the angle of incidence between the photon and the sensing area; with the fiber optic sensors this is accomplished by modifying the geometry of the probe tip: different incident angle produces different resonance wavelength, therefore, for the refractive index variety, different incident angle produces different resonance wavelength range, which also names dynamic range. Here we propose a fiber butt-joint method to adjust the SPR incident angle. Figure 1 shows the sketch diagram of the twin-core fiber (TCF) SPR sensor probe. We polish the fiber I with the angle of α, and polish the fiber II with the same grinding angle. Then we splice two fibers together keeping the core I-2 in fiber I arranging with the core II-2 in the fiber II. We plate a 50nm gold film on the inclined plane I to configure the Kretschmann prism structure. When the light beam is launched into the core I-1, it is totally internal reflected on the inclined plane I and a SPR generating on the 50nm gold film, then the SPR sensing signal, which is carried by the reflected light beam, will be totally internal reflected by the 300nm gold film on the inclined plane II, and then entering the core II-1 of the fiber II. Finally the SPR sensing information is received by the optical spectrum analyzer.

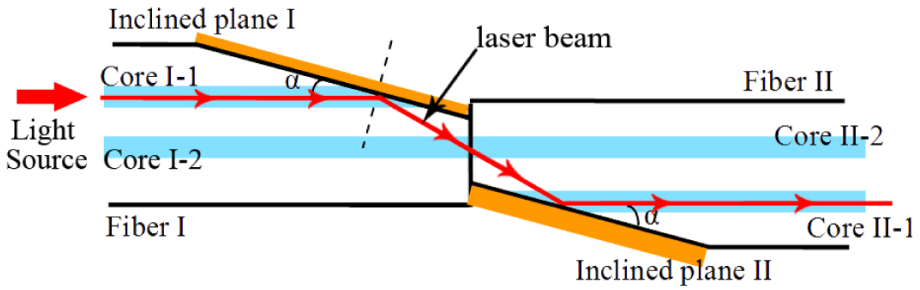

Fig. 1. Sketch diagram of incident angle adjusting method.

Dynamic range adjustment: Taking the grinding angle of 7° and 16° as the example, we test and verify the method of separating the dynamic range. Figure 2 shows the simulated and experimental results. According to the Figs. 2(a) and 2(c), when the fiber grinding angle is 7°(resonance angle is 83°), the dynamic range is 604~713nm and the sensitivity is 2096nm/RIU; when the fiber grinding angle is 16°(resonance angle is 74°), the dynamic range is 702~1128nm and the sensitivity is 8192 nm/RIU. According to the Figs. 2(b) and 2(d), when the grinding angle is 7°, the testing dynamic range is 585~692nm and the testing sensitivity is 2058 nm/RIU; when the fiber grinding angle is 16°, the testing dynamic range is 744~908nm and the testing sensitivity is 3905nm/RIU. Here, the testing scope of our optical spectrum

#246622 Received 28 Jul 2015; revised 31 Aug 2015; accepted 1 Sep 2015; published 3 Sep 2015
(C) 2015 OSA

analyzer is 0~1000nm, therefore the resonance dip of the "1.385 index" curve cannot be recorded in the Fig. 2(d), the "908nm" is the resonance wavelength of the "1.375 index", and the corresponding simulated results is 973nm (see Fig. 2(c)). Consequently, compared with the simulated results and the experimental results, we can separate the SPR dynamic range by changing the fiber grinding angle. The simulated conditions are: the refractive index of the fiber core is 1.467, the gold film thickness is 50nm, and the dielectric constant of the gold film is referenced from [22].

Therefore, we can realize the series connecting SPR sensing by polishing the fiber with the angle of 7° and 16°, the dynamic range of two sensing channels can be separated completely, the two dynamic ranges are 585~692nm and 744~908nm.

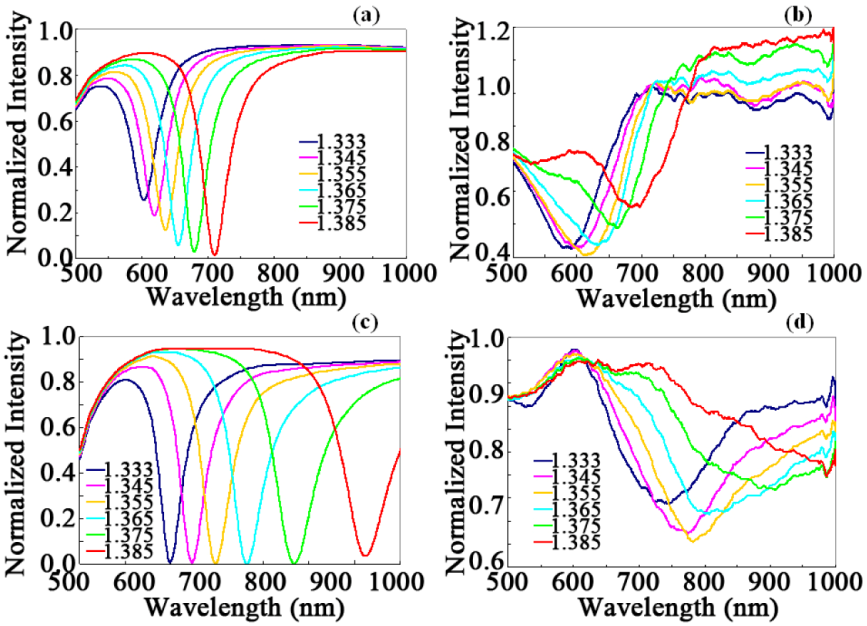

Fig. 2. (a) simulated results of fiber grinding angle of 7° ; (b) experimental results of fiber grinding angle of 7° ; (c) simulated results of fiber grinding angle of 16° ; (d) experimental results of fiber grinding angle of 16°.

2.2 Realization of TDM (parallel-connection sensor)

In order to realize the TDM technology applied in the distributed fiber-based SPR sensor, which means realizing the parallel connection of two sensing passages, we employ the twin-core fiber, which means we integrate two sensing passages into a same fiber to realize the series connection of two sensing passages.

According to the Fig. 2, the larger is the fiber grinding angle, the smaller is the SPR resonance angle, the higher is the sensor sensitivity, and the dynamic range is red-shift. Therefore, by using the two cores in the twin-core fiber, we configure a twin-passage four-channel SPR sensor. For sensing passage I, we polish the fiber with the angle of 7°(channel I-1) and 16°(channel I-2), and for sensing passage II, we polish the fiber with the angle of 11°(channel II-1) and 18°(channel II-2). Therefore, we realize the series connection of channel I-1 and channel I-2, the series connection of channel II-1 and channel II-2, and the parallel connection of passage I and passage II in a same fiber. Figure 3 shows the sketch diagram of the twin-passage four-channel SPR sensor.

#246622 Received 28 Jul 2015; revised 31 Aug 2015; accepted 1 Sep 2015; published 3 Sep 2015
(C) 2015 OSA

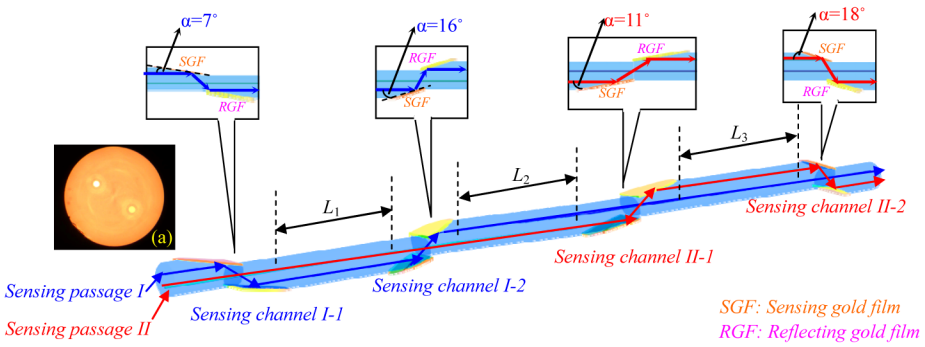

Fig. 3. Sketch diagram of twin-passage four-channel SPR sensor based on the twin-core fiber; (a) profile image of the twin-core fiber

Figure 3(a) shows the profile of the twin-core fiber. The core diameter of the twin-core fiber is 8μm, the cladding diameter is 125μm and the distance between the two cores is 62.5μm. Due to the size of the fiber core, there are few modes beam propagating during 500~2400nm, which is the super continuum light source spectrum wide.

Therefore, by using the twin-core fiber, we employ the TDM technology to realize the distributed multichannel parallel-connection (twin-passage) sensing, and by using the fiber end polishing and connecting method, we employ the WDM technology to realize the distributed multichannel series-connection (four-channel) sensing. We integrate two passages four channels sensing in a same fiber.

3. Experiments

3.1 fabrication of sensing zone

The processing steps of the twin-passage four-channel fiber sensor are:

(1) *Fiber polishing*: the roughness of the angled face of the fiber strongly affect the performance of generating the SPR in this scheme. If the angled face is rough, there will be more than one SPR incident angle, which will cause the SPR resonance dips broadening and sensitivity reducing. Therefore, in order to make the angled face as smooth as possible, we polish the twin-core fiber (TCF) to be the designed angle and depth by using a fiber grinding machine. We grind the fiber with a 8000-grit grinded paper for 2 hours, and then polish it with a 12000-grit polished paper to make sure the polished plane completely flat (see Fig. 4(a), where α is 16°);

(2) *Fiber fusing*: We connect with two polished TCFs by using a fiber splicer. One fiber holder in the splicer clamps the first TCF, while the other holder clamps the second TCF simultaneously, and then the second fiber holder rotates the second TCF to arrange two fibers as we wanted position, and then fusing two fibers with a suitable fusing parameter(seen Fig. 4(b));

(3) *Gold film coating*: We employ the vacuum plasma sputtering method to plate the gold film on the fiber. Here we place the connected fiber in the vacuum chamber of the plasma sputtering apparatus(JS-1600, HTCY©) to plate the sensing gold film (50nm) on the first fiber and then overturn the connected fiber to plate the reflected gold film (300nm) on the second fiber. We adjust the thickness of the gold film by controlling the sputtering current and sputtering time. The gold film thickness is measured by using the three-dimensional morphology analyzer (NewView7200, Zygo). The gold film is scratched as line shape. The flatness of gold film surface and the depth of the groove are observed by the morphology analyzer (seen Fig. 4(c) and 4(d)). The depth of the groove indicates the thickness of the coated gold film.

#246622 Received 28 Jul 2015; revised 31 Aug 2015; accepted 1 Sep 2015; published 3 Sep 2015
(C) 2015 OSA

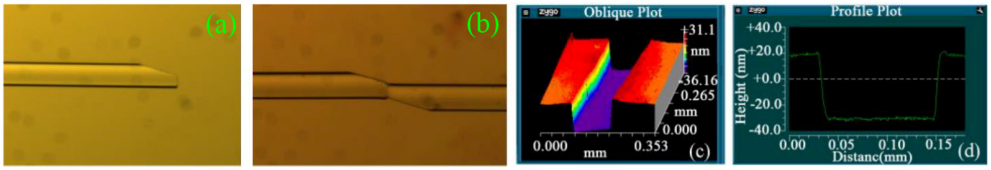

Fig. 4. (a) Image of the first TCF with the grinding angle α of 16°; (b) image of the fused two TCFs; (d) the three dimensional testing result of the gold film surface with a groove; (e) the test result of the groove depth, which equals to the film thickness.

3.2 Experimental setup

The experimental setup is shown in the Fig. 5. A super continuum light source (SuperK compact, NKT Photonics) whose spectrum wide is 500~2400nm, is launched into one core of the TCF by using a beam alignment device, and the reflected beam is received by an optical spectrum analyzer (AQ6370C, Yokokawa). A beam alignment device is employed to realize the light source power switch between the two cores. At first, the light source power is launched from a normal single mode fiber (SMF) into the core I of the TCF to make the sensing passage I working, and then the light source power is switched to the core II to make the sensing passage II working. We employ a programmable micro injection pumper (LSP01-1A, LongerPump) to inject the Glycerine-aqueous solution into the micro fluidic channels. The Glycerine-aqueous solution index is calibrated by the Abbe refractometer (GDA-2S, Gold).

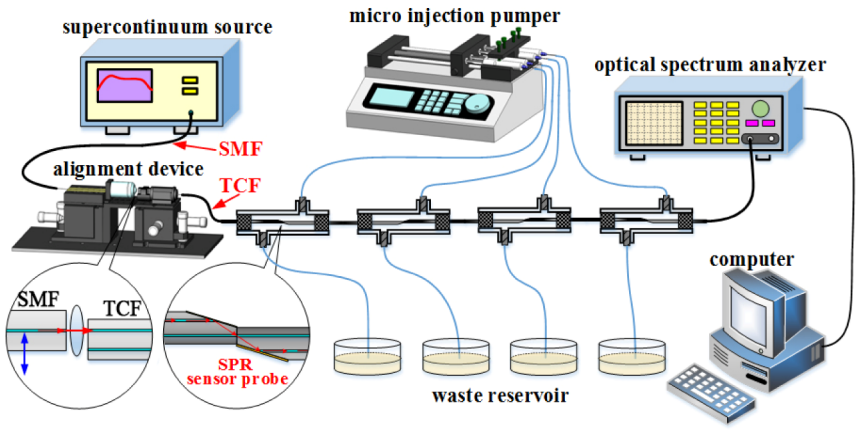

Fig. 5. The experiment setup sketch diagram of the twin-core fiber SPR sensor

4. Results and discussion

4.1 Simulated and experimental results of sensing passage I

Figures 6(a) and 6(b) provide the simulated and experimental results of the transmitted attenuating spectrum keeping the sensing channel I-2 in the Glycerine-aqueous solution with the refractive of n = 1.365 and placing the sensing channel I-1 in the Glycerine-aqueous solution with index of 1.333, 1.345, 1.355, 1.365 1.375 and 1.385 successively. From the experimental results, the dips generated from the sensing channel I-1 is unchanged (keeping in 824nm), and the dips generated from the sensing channel I-2 move from 586nm to 705nm, and the testing sensitivity is 2288nm/RIU, which is consistent with the simulated results. Although the amplitude of the transmitted attenuating spectrum is not consistent with the simulated results, here we investigate the position of the resonance dip, which is consistent with the simulated results.

#246622 Received 28 Jul 2015; revised 31 Aug 2015; accepted 1 Sep 2015; published 3 Sep 2015
(C) 2015 OSA

Similarly, Figs. 6(c) and 6(d) provide the simulated and experimental results of the transmitted attenuating spectrum keeping the sensing channel I-1 in the water (n = 1.333) and placing the sensing channel I-2 in the Glycerine-aqueous solution with index of 1.333, 1.345, 1.355, 1.365 and 1.375 successively(here, due to the limited optical spectrum analyzer testing range, we do not test the index of 1.385). From the experimental results, the dips generated from the sensing channel I-1 is unchanged (keeping in 586nm), and the dips generated from the sensing channel I-2 move with the range of 731~894nm, and the testing sensitivity is 3881nm/RIU, which is also consistent with the simulated results.

Figures 6(e) and 6(f) provides the simulated and experimental results of the transmitted attenuating spectrum placing both sensing channel I-1 and I-2 in the Glycerine-aqueous solution with the same index range. From the experimental results, the testing resonance range of sensing channel I-1 is 584~695nm with the sensitivity of 2235nm/RIU, while the testing resonance range of sensing channel I-2 is 738~914nm with the testing sensitivity is 4190nm/RIU. Here due to the testing scope of the optical spectrum analyzer is 0~1000nm, the corresponding testing range of the refractive index is 1.333~1.375, however, the experimental results are consistent with the simulated results.

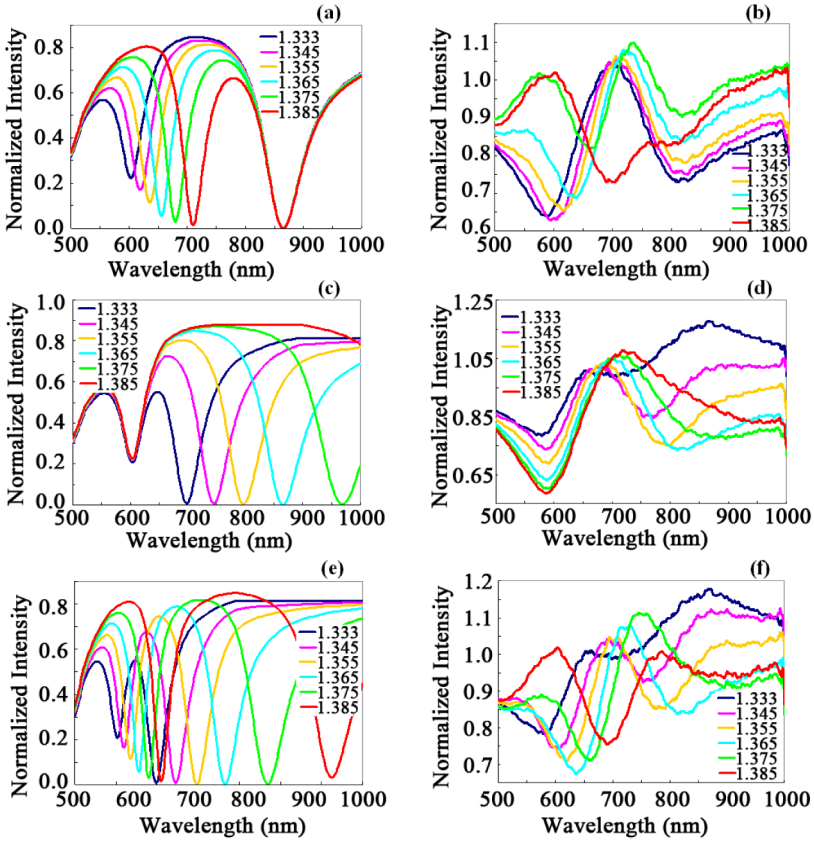

Fig. 6. (a) Simulated and (b) experimental results of the SPR spectrum with only sensing channel I-1 working; (c) simulated and (d) experimental results of the SPR spectrum with only sensing channel I-2 working; (e) simulated and (f) experimental results of the SPR spectrum with both sensing channels in passage I working.

4.2 Simulated and experimental results of sensing passage II

Similarly we test the sensing passage II. Adjusting the position of the SMF in the beam alignment device (see Fig. 5), switching the light source power launching from core I to the

#246622 Received 28 Jul 2015; revised 31 Aug 2015; accepted 1 Sep 2015; published 3 Sep 2015
(C) 2015 OSA

core II, then sensing passage II works, and the Fig. 7(a) and 7(b) shows the simulated and experimental results, showing the transmitted attenuating spectrum placing both sensing channel II-1 and channel II-2 in the Glycerine-aqueous solution with the index range 1.333~1.385 and 1.333~1.375 respectively. From the experimental results, the testing resonance range of sensing channel II-1 is 635~776nm with the sensitivity of 2712nm/RIU, while the testing resonance range of sensing channel II-2 is 743~958nm with the testing sensitivity is 5119nm/RIU. Here due to the testing scope of the optical spectrum analyzer is 0~1000nm, the resonance dip of the "1.385 index" curve cannot be recorded in the Fig. 7(b), the corresponding testing range of the refractive index is 1.333~1.375, however, the experimental results are consistent with the simulated results.

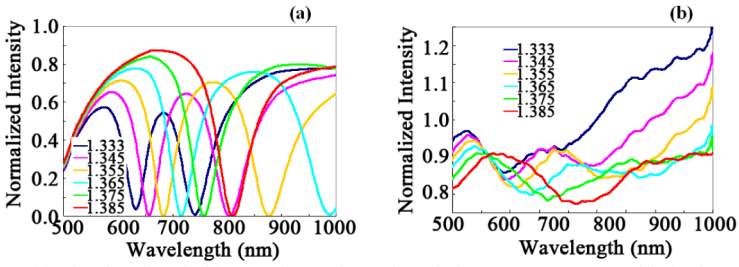

Fig. 7. (a) simulated and (b) experimental results of the SPR spectrum with both sensing channels in passage II working.

Unlike some traditional cascaded fiber sensors [18–21], who have to abandon the testing sensitivity to realize the cascaded configuration, this twin-passage four-channel sensor can keep the high sensitivity in the cascaded configuration. Figure 8 shows the comparison of the sensitivity (the slope of the curves in the Fig. 8 equals to the sensitivity). Here SS means the experimental results of a normal Single Sensor; SMCS means the experimental results of Single sensing zone of the Multi-Channel Sensor, DMCS means the experimental results of the Double sensing zones of the Multi-Channel Sensor. According to the Fig. 8, the testing sensitivity of the each sensing zone keeps the same as the normal single sensor(SS).

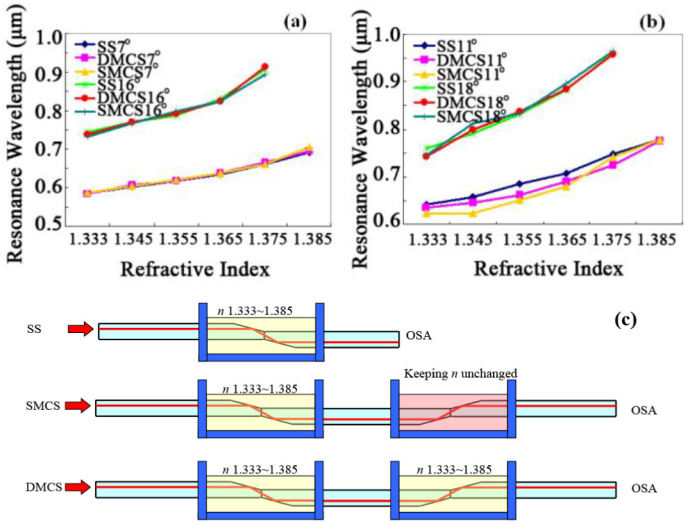

Fig. 8. Comparison of the testing sensitivity with different working function of (a) sensing passage I and (b) sensing passage II; (c) the sketch diagram of the wording function of one sensing passage (sensing passage I or sensing passage II), here OSA means optical spectrum analyzer.

#246622 Received 28 Jul 2015; revised 31 Aug 2015; accepted 1 Sep 2015; published 3 Sep 2015
(C) 2015 OSA

5. Conclusion

In summary, a twin-passage four-channel SPR sensor based on the twin-core optical fiber is proposed. The twin-passage four-channel in the sensor is realized by cascading four sensing units with different fiber grinding angles. The overview of the experimental results are shown in the Table 1. In the sensing passage I (the fiber grinding angles are 7° and 16°), the testing sensitivities are 2235nm/RIU and 4190nm/RIU during the refractive index range of 1.333~1.385; In the sensing passage II (the fiber grinding angles are 11° and 18°), the testing sensitivities are 2712nm/RIU and 5119nm/RIU during the same refractive index range.

Tab.1 Overview of the experimental results

TDM technology	⇨	Sensing Passage I		Sensing Passage II	
WDM technology	⇨	Channel I-1	Channel I-2	Channel II-1	Channel II-2
Resonance angle	(°)	7	16	11	18
Dynamic range	(nm)	584~695	738~914	635~776	743~958
Sensitivity	(nm/RIU)	2235	4190	2712	5119

According to the working principle above, we can easily infer that there are two working ways of this twin-passage four-channel SPR sensor: (1) Alternating working (passage I on with passage II off or passage I off with passage II on): the sensing passage I and sensing passage II work independently by switching light source power into two cores; (2) Simultaneous working (passage I on with passage II on): the sensing passage I and sensing passage II work simultaneously by using two light sources and two optical spectrum analyzers. Therefore, this four-channel SPR sensor can be used to detect multiple analytes simultaneously by using alternating working way, and also can be used to the multiple analytes self-reference measurement by using simultaneous working way.

We have to admit that, due to the geometrical structure of the twin-core fiber, (the distance between the two cores is 62.5μm,) there is a large insertion loss, ~70%, between the two fibers. Therefore normally, there are two cascaded structure at most. However, in a practical distributed SPR sensor, in a sensing passage, 2~3 sensing zones are enough, too many cascades sensing zones will cause the resonance dips overlapping, which will effect the sensor performance.

This SPR sensor constitutes a new development for distributed SPR sensors which keeps the high testing sensitivity. Besides that, it is convenient for this twin-passage four-channel SPR sensor to control the distributed distance and realize the self-reference measurement. This SPR sensor is expected to be employed by monitoring the glucose, cholesterol, hemoglobin, urea, PH and other useful indicators in a small amount of blood. It can help to compensate or eliminate the interference from the background refractive index, physical absorption and other factors.

Acknowledgments

This work is supported by the National Natural Science Foundation of China (Grants No. 61405043, 11204047, 61227013, 61275087, 61205071 and 61377085), and partially supported by the following grants: the 111 project (B13015), Postdoctoral Science Foundation Fund of China (Grants No. 2014M550181, 2014M551217), the Natural Science Foundation of Heilongjiang Province (F201405) and Fundamental Research Funds for Harbin Engineering University of China.